ISSN 1674-1056
http://cpb.iphy.ac.cn
http://iopscience.iop.org/cpb
中国物理 B
Chinese Physics
中国物理 Chinese Physics B

Crystallographic and magnetic properties of van der Waals layered $FePS_3$ crystal

Qi-Yun Xie(解其云), Min Wu(吴敏), Li-Min Chen(陈丽敏), Gang Bai(白刚), Wen-Qin Zou(邹文琴), Wei Wang(王伟), Liang He(何亮)

Citation: Chin. Phys. B . 2019, 28(5): 056102. **doi:** 10.1088/1674-1056/28/5/056102
Journal homepage: http://cpb.iphy.ac.cn; http://iopscience.iop.org/cpb

What follows is a list of articles you may be interested in

Review of improved spectral response of ultraviolet photodetectors by surface plasmon

You Wu(吴忧), Xiao-Juan Sun(孙晓娟), Yu-Ping Jia(贾玉萍), Da-Bing Li(黎大兵)

Chin. Phys. B . 2018, 27(12): 126101. **doi:** 10.1088/1674-1056/27/12/126101

Effects of Al component content on optoelectronic properties of $Al_xGa_{1-x}N$

Yan-Jun Ji(纪延俊), Jun-Ping Wang(王俊平), You-Wen Liu(刘友文)

Chin. Phys. B . 2018, 27(10): 106102. **doi:** 10.1088/1674-1056/27/10/106102

Synthesis of Pr-doped ZnO nanoparticles: Their structural, optical, and photocatalytic properties

Jun-Lian Chen(陈军联), Neena Devi, Na Li(李娜), De-Jun Fu(付德君), Xian-Wen Ke(柯贤文)

Chin. Phys. B . 2018, 27(8): 086102. **doi:** 10.1088/1674-1056/27/8/086102

Synthesized few-layers hexagonal boron nitride nanosheets

Zhao-Jun Mo(莫兆军), Zhi-Hong Hao(郝志红), Xiao-Jie Ping(平晓杰), Li-Na Kong(孔丽娜), Hui Yang(杨慧), Jia-Lin Cheng(程佳林), Jun-Kai Zhang(张君凯), Yong-Hao Jin(金永昊), Lan Li(李岚)

Chin. Phys. B . 2018, 27(1): 016102. **doi:** 10.1088/1674-1056/27/1/016102

Mechanical properties of self-irradiated single-crystal copper

Li Wei-Na, Xue Jian-Ming, Wang Jian-Xiang, Duan Hui-Ling

Chin. Phys. B . 2014, 23(3): 036101. **doi:** 10.1088/1674-1056/23/3/036101

Crystallographic and magnetic properties of van der Waals layered $FePS_3$ crystal*

Qi-Yun Xie(解其云)[1,4], Min Wu(吴敏)[1], Li-Min Chen(陈丽敏)[1], Gang Bai(白刚)[1], Wen-Qin Zou(邹文琴)[3], Wei Wang(王伟)[2,3,†], and Liang He(何亮)[3,‡]

[1] *Key Laboratory of Radio Frequency and Micro-Nano Electronics of Jiangsu Province, Nanjing University of Posts & Telecommunications, Nanjing* 210023, *China*

[2] *Key Laboratory of Flexible Electronics (KLOFE) & Institute of Advanced Materials (IAM), Jiangsu National Synergetic Innovation Center for Advanced Materials (SICAM), Nanjing Tech University, Nanjing* 211816, *China*

[3] *Jiangsu Provincial Key Laboratory of Advanced Photonic and Electronic Materials, Collaborative Innovation Center of Advanced Microstructures, School of Electronic Science and Engineering, Nanjing University, Nanjing* 210093, *China*

[4] *National Laboratory of Solid State Microstructures, Nanjing University, Nanjing* 210093, *China*

(Received 23 November 2018; revised manuscript received 26 February 2019; published online 20 March 2019)

The crystallographic and magnetic properties are presented for van der Waals antiferromagnetic $FePS_3$. High-quality single crystals of millimeter size have been successfully synthesized through the chemical vapor transport method. The layered structure and cleavability of the compound are apparent, which are beneficial for a potential exploration of the interesting low dimensional magnetism, as well as for incorporation of $FePS_3$ into van der Waals heterostructures. For the sake of completeness, we have measured both direct current (dc) and alternating current (ac) magnetic susceptibility. The paramagnetic to antiferromagnetic transition occurs at approximately $T_N \sim 115$ K. The effective moment is larger than the spin-only effective moment, suggesting that an orbital contribution to the total angular momentum of the Fe^{2+} could be present. The ac susceptibility is independent of frequency, which means that the spin freezing effect is excluded. Strong anisotropy of out-of-plane and in-plane susceptibility has been shown, demonstrating the Ising-type magnetic order in $FePS_3$ system.

Keywords: $FePS_3$, van der Waals crystals, single crystal, antiferromagnetism

PACS: 61.72.uj, 75.50.Ee, 78.67.Bf **DOI:** 10.1088/1674-1056/28/5/056102

1. Introduction

The discovery of graphene in 2004[1] has opened up intense research of various two-dimensional (2D) materials, such as transition-metal dichalcogenides,[2] black phosphorus,[3] hexagonal boron nitride,[4] InSe,[5] etc. The studies on these materials as well as stacked heterostructures[6,7] based on them have revealed interesting properties and potential applications. Despite the vast family of 2D crystals, only a few exhibit intrinsic magnetic orders. The discovery of suitable 2D magnetic materials holds promise for future nanoelectronics and spintronic applications. Therefore, recently some investigations on ferromagnetic CrI_3,[8] $Cr_2Ge_2Te_6$,[9] and antiferromagnetic transition-metal trichalcogenides with the chemical formula of MPX_3[10,11] have been reported.

Among all the predicted and experimentally observed antiferromagnetic transition-metal trichalcogenides, a very promising material of particular interest is $FePS_3$. There have been many studies of $FePS_3$ since its discovery,[12–16] not only in the field of spintronics,[17,18] but also in the areas of catalyst chemistry[19] and electronic devices. For example, Raman spectroscopy measurements show the Ising-type antiferromagnetic order can even survive down to the monolayer limit.[20] $FePS_3$ quantum sheets demonstrate a substantially accelerated photocatalytic H_2 generation rate, which is up to three times higher than the bulk counterpart.[21] Both negative and positive photoconductivity exist in $FePS_3$-based photodetectors and can be controllably switched with bias voltage.[22] Existing studies make $FePS_3$ an ideal candidate for 2D magnetic as well as optoelectronic systems. However, the corresponding research is still in its infancy, which motivates us to deeply investigate the crystallographic and magnetic properties of $FePS_3$ using various experimental characterization methods.

In this work, the chemical vapor transport (CVT) route, which has been considered as a promising way to synthesize layered materials, is utilized to grow $FePS_3$ with high quality in a large scale. The as-grown crystals show highly anisotropic magnetic properties. The frequency-independent behavior of alternating current (ac) magnetic susceptibility rules out the spin freezing. Instead, they represent the clear antiferromagnetic phase transition and the magnetic ordering is of Ising-

*Project supported by the National Natural Science Foundation of China (Grant Nos. 11404169, 51602159, and 11704196), the Scientific Research Foundation of Nanjing University of Posts & Telecommunications, China (Grant Nos. NY217043 and NY218021), and the Postgraduate Research & Practice Innovation Program of Jiangsu Province, China (Grant Nos. KYCX17_0754 and SJCX18_0287).

†Corresponding author. E-mail: wwesun2000@163.com

‡Corresponding author. E-mail: heliang@nju.edu.cn

© 2019 Chinese Physical Society and IOP Publishing Ltd

type.

2. Experiment

High quality single crystals of $FePS_3$ were grown by a typical CVT method. The stoichiometric amount high purity elements (99.99% Fe, 99.999% P, and 99.999% S from Alfa Aesar) and iodine as the transport agent were placed in a quartz ampoule and sealed under vacuum. The ampoule was further placed in a horizontal 2-zone furnace. The temperatures were set at 750 °C (hot zone) and 650 °C (cold zone) and kept at that condition for 21 days. The quality of crystals was characterized by a Rigaku Dmax-rB diffractometer with Cu $K\alpha$ radiation. A scanning electron microscope (SEM) equipped with an energy dispersive spectroscopy (EDS) was used to check the surface morphology and composition ratio of the synthesized crystals. The microstructure of crystals was also observed by transmission electron microscopy (TEM) and selected area electron diffraction (SAED) using JEM-200CX microscope. For the study of Raman spectra, a He–Ne laser ($\lambda = 488$ nm) was used as the excitation beam. The x-ray photoelectron spectroscopy (XPS) spectra were obtained using PHI 5000 VersaProbe instrument. The direct current (dc) magnetizations from 300 K to 10 K were measured with a superconducting quantum interference device (SQUID) magnetometer (Quantum Design) under a magnetic field of 500 Oe, and the low temperature ac magnetic susceptibility was measured by physical property measurement system (PPMS, Quantum Design).

3. Results and discussions

In $FePS_3$ crystal, the magnetic Fe atoms form a honeycomb arrangement and each of them is octahedrally coordinated by six S atoms with a small trigonal distortion. The P atom is coordinated with three S atoms and one P atom to form a $[P_2S_6]^{4-}$ unit. The S atomic layers are arranged along the c direction in an *ABCABC* stacking sequence, forming in a monoclinic structure with the space group of $C2/m$. The layered nature is apparent from the crystal structure in Fig. 1(b), where the topography of van der Waals gap separating layers is visible. Hence, it is possible to make $FePS_3$ easily exfoliated by scotch tape.

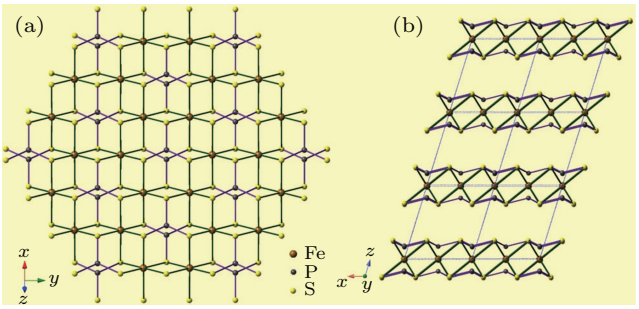


Fig. 1. (a) In-plane and (b) out-of-plane crystal structures of $FePS_3$.

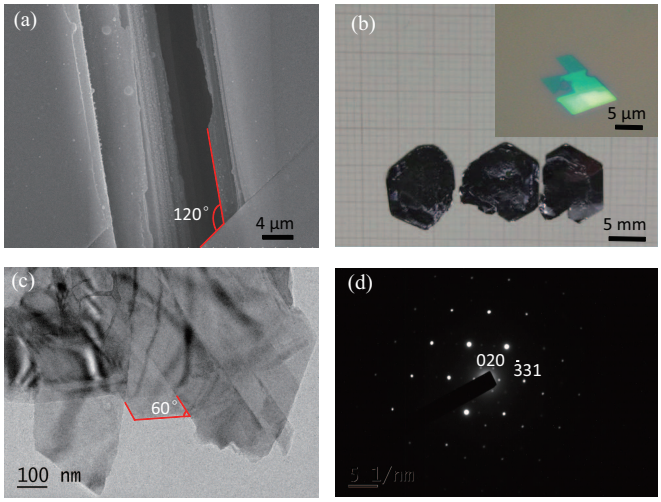


Fig. 2. (a) SEM image, (b) photo of bulk $FePS_3$ crystals, and the typical exfoliated $FePS_3$ (the inset in (b)). The bright-field TEM image and electron diffraction pattern are shown in (c) and (d), respectively.

In our study, the CVT method has been shown to successfully yield high quality $FePS_3$ crystals. A typical SEM image of as-grown crystal is shown in Fig. 2(a), exhibiting the expected layered structure. As mentioned above, $FePS_3$ has a hexagonal in-plane structure. So, the straight edges with characteristic inner angles of $\sim 120°$ can be easily identified in the morphology. Most of the obtained $FePS_3$ flakes have an average size of about 10 mm, as shown in Fig. 2(b). The parameters of cleavage energy and cleavage strength are normally utilized to estimate the possibility of mechanical exfoliation from the bulk 2D van der Waals. Previously, it has been shown that the cleavage energy of $FePS_3$ is comparable to the experimentally estimated value of graphite and the cleavage strength is even lower than that of graphite,[23] which indicates that the exfoliation of bulk $FePS_3$ by scotch tap methods is feasible. Here, we have mechanically exfoliated the as-grown bulk $FePS_3$ crystal onto freshly cleaned Si substrates with a 300-nm-thick SiO_2 top-layer (see the inset of Fig. 2(b)). The resulting $FePS_3$ sheets show different optical contrast due to the interference. Different colors represent different thicknesses. The preferential crack-propagation along the high-symmetry crystal axis during exfoliation results in typical 120° or 60° angles between sheet edges.[24] The successful achievement of ultrathin $FePS_3$ favors for exploring the interesting low dimensional magnetism, as well as for further incorporation $FePS_3$ into van der Waals heterostructures. The chemical compositions of $FePS_3$ have been measured by EDS, which reveals that the ratio of Fe:S:P is very close to the expected 1:1:3, suggesting the formation of $FePS_3$ phase. The TEM morphology image is shown in Fig. 2(c), demonstrating the 2D nanosheet-like geometry of $FePS_3$. It seems that there are wrinkles in the sample. The SAED pattern is taken with the incident electron beam normal to the *ab*-plane. Well-defined diffraction spots are clearly shown, confirming the presence of characteristic

planes. Our SAED pattern agrees well with that reported by Murayama *et al.*,[25] suggesting that the prepared crystals are likely to have rotational twins and are pseudo-3-fold symmetrical.

The x-ray diffraction (XRD) data are further collected at room temperature to determine the orientation of the as-grown crystals. As shown in Fig. 3(a), only $(00l)$- oriented peaks for monoclinic structure (PDF#30-0663) of $FePS_3$ appear without any other impurities peaks, exhibiting high crystalline phase purity as well as the desired layer structure. Structural characterization has also been performed by Raman spectroscopy. The Raman spectra at room temperature are collected using a 488 nm laser. On the basis of the present experiments and of previous analysis, the Raman peaks can be assigned as follows. The peak around 100 cm^{-1} originates from the Fe atom vibrations. This peak is a spin-disorder-induced mode and could be replaced by other spin-order-induced modes below the Néel temperature of $FePS_3$.[26] The peak around 155 cm^{-1} is the strongly infrared (IR) active E_u type mode of the P_2S_6 molecule, which can be observed in all the MPS_3 compound.[27] The other peaks come from $[P_2S_6]^{4-}$ anion vibrational modes. The Raman peaks at 247 cm^{-1} and 380 cm^{-1} correspond to the A_{1g} mode, which is the out-of-plane vibration of P_2S_6 entities. The other three peaks observed at 227 cm^{-1}, 279 cm^{-1}, and 579 cm^{-1} are related to the E_g mode. Overall, the Raman modes observed in our experiment agree well with previous studies.[15,26,27] The careful studies on thickness dependence and temperature dependence of Raman spectra for $FePS_3$ are underway.

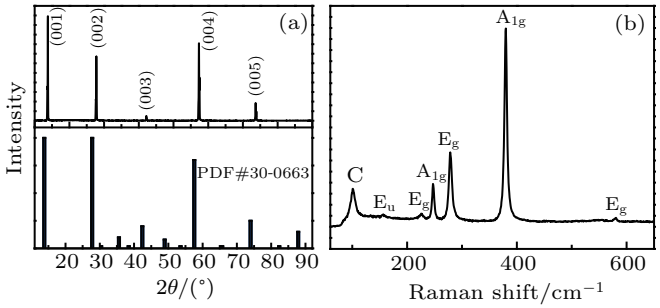


Fig. 3. (a) X-ray diffraction pattern and (b) Raman spectrum of the as-grown $FePS_3$ measured at room temperature.

The surface sensitive XPS has been performed to detect the surface composition and chemical state of $FePS_3$. The atomic ratio of Fe:S:P is detected to be also about 1:1:3. The corresponding Fe 2p, P 2p, and S 2p XPS spectra are shown in Fig. 4. The Fe 2p spectra appear as well-resolved doublets. The Fe^{2+} state can be ascertained from the peaks of Fe $2p_{1/2}$ and Fe $2p_{3/2}$ at the binding energies of 722 eV and 709 eV. The two resolved S 2p peaks at 162.4 eV and 163.5 eV are assigned to $2p_{1/2}$ and $2p_{3/2}$, respectively, implying Fe–S and P–S entities. The P 2p peaks located at 131.9 eV and 132.5 eV correspond to P $2p_{1/2}$ and P $2p_{3/2}$, respectively. All the values are comparable with previous reported values.[19,28]

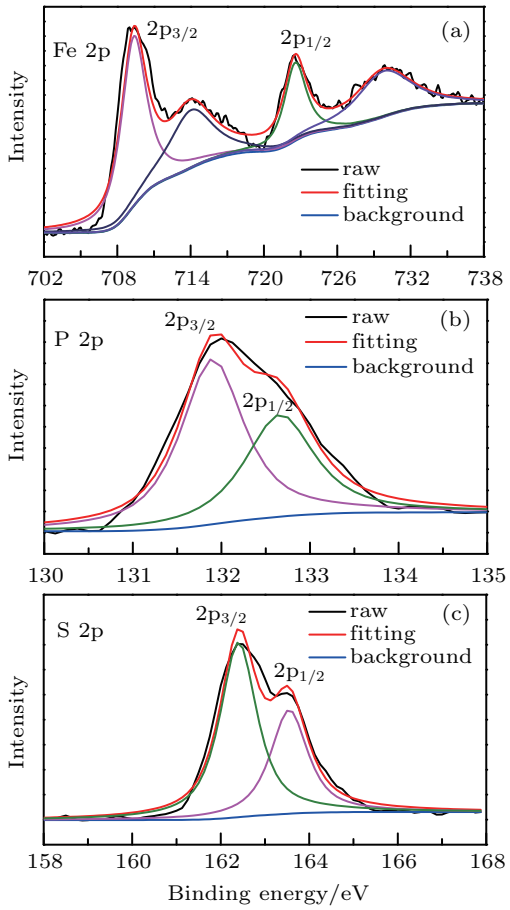


Fig. 4. XPS spectra of (a) Fe 2p, (b) P 2p, and (c) S 2p for $FePS_3$.

In addition to structural characterization, the magnetic properties of $FePS_3$ crystals have been further probed. The dc magnetic susceptibilities χ, measured with the 500 Oe field along the layer stacking direction ($\chi_\perp$, out-of-plane) and with the field in the plane of the $FePS_3$ layers ($\chi_\parallel$, in-plane), are shown in Fig. 5(a). The curves show clear magnetic phase transition from the antiferromagnetic to paramagnetic phase around Néel temperature. The first derivative of susceptibility curves indicates a transition temperature of $\sim$ 115 K, which is in agreement with previous studies.[20,26] Moreover, considerable anisotropy of χ is apparent. The change of χ out of plane is much larger than that in plane, implying that the spin is aligned along the out-of-plane direction. The anisotropy in $FePS_3$ is so strong that it will create an energy gap of $\sim$ 16 meV in the spin-wave spectrum.[29] The high-temperature paramagnetic susceptibility in both directions obeys the Curie–Weiss law $\chi = C/(T - T_C)$, where C is the Curie constant from which the effective magnetic moment μ_{eff} of Fe^{2+} could be deduced, and T_C is the Curie temperature. Fitting the data at high temperature gives an effective moment of $\mu_{eff} = 6.02\ \mu_B$, $T_C = 62$ K for $\chi_\perp$, and $\mu_{eff} = 5.23\ \mu_B$, $T_C = -85$ K for $\chi_\parallel$, respectively. The different sign of T_C is

probably associated with the crystal-field effects arising due to the trigonal elongation of the FeS_6 octahedra.[30] If we consider the spin of Fe ion only, the theoretical $\mu_{\rm eff}$ would be 4.9 $\mu_{\rm B}$. The values after fitting are larger than the spin-only effective moment, which has also been reported in the previous studies.[30,31] This might indicate that the orbital momentum in $FePS_3$ is not completely quenched.[30] However, more studies are still needed in the future to give direct evidences. The temperature dependence of the out-of-plane ac susceptibility $\chi_{\rm ac}$ under different frequencies is also shown in Fig. 5(b). Over the entire range of measured frequencies from 100 Hz to 2000 Hz, no frequency dispersion is observed, which rules out a spin freezing transition.

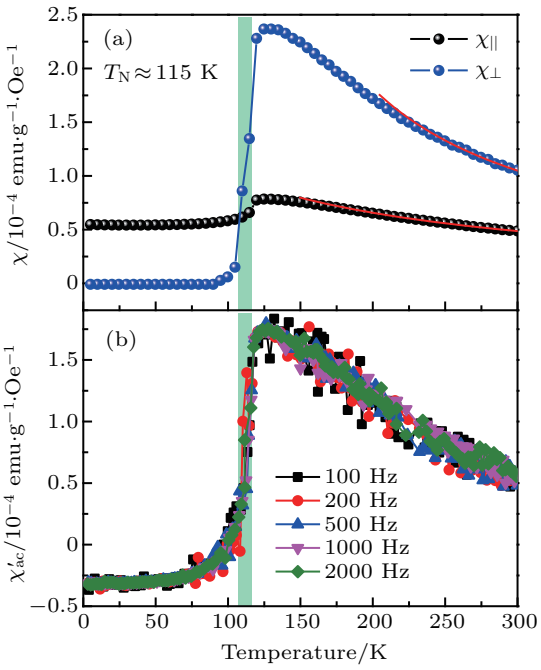


Fig. 5. (a) Temperature dependence of dc parallel ($\chi_{\parallel}$) and perpendicular ($\chi_{\perp}$) magnetic susceptibility of $FePS_3$. The fitting curve using the Curie–Weiss law is also shown. (b) Temperature dependence of real ac magnetic susceptibility of $FePS_3$ measured at different frequencies from 100 Hz to 2000 Hz.

4. Conclusions

A comprehensive study of crystallographic and magnetic properties of high quality van der Waals layered $FePS_3$ single crystals has been performed using SEM, TEM, XRD, Raman, XPS, $\chi_{\rm dc}(T)$, and $\chi_{\rm ac}(T)$. The synthesized $FePS_3$ show single-crystallinity with the average size of about 10 mm. The crystals can be exfoliated down to few layers. The preferred cleavage angles are 120 degrees or 60 degrees. $FePS_3$ exhibits typical magnetic transition from the paramagnetic to antiferromagnetic phase. The derived effective moments are larger than the spin-only effective moment, suggesting that an orbital contribution to the total angular momentum of the Fe^{2+} could be present. The ac susceptibility lacks frequency dependence, which means that the spin freezing effect is excluded.

References

[1] Novoselov K S, Geim A K, Morozov S V, Jiang D, Zhang Y, Dubonos S V, Grigorieva I V and Firsov A A 2004 *Science* **306** 666

[2] Radisavljevic B, Radenovic A, Brivio J, Giacometti V and Kis A 2011 *Nat. Nanotechnol.* **6** 147

[3] Li L K, Yu Y J, Ye G J, Ge Q Q, Ou X D, Wu H, Feng D L, Chen X H and Zhang Y B 2014 *Nat. Nanotechnol.* **9** 372

[4] Dean C R, Young A F, Meric I, Lee C, Wang L, Sorgenfrei S, Watanabe K, Taniguchi T, Kim P, Shepard K L and Hone J 2010 *Nat. Nanotechnol.* **5** 722

[5] Li Y, Wang T M, Wu M, Cao T, Chen Y W, Sankar R, Ulaganathan R K, Chou F C, Wetzel C, Xu C Y, Louie S G and Shi S F 2018 *2D Mater.* **5** 021002

[6] Lee C H, Lee G H, van der Zande A M, Chen W, Li Y, Han M, Cui X, Arefe G, Nuckolls C, Heinz T F, Guo J, Hone J and Kim P 2014 *Nat. Nanotechnol.* **9** 676

[7] Joo M K, Moon B H, Ji H, Han G H, Kim H, Lee G, Lim S C, Suh D and Lee Y H 2016 *Nano Lett.* **16** 6383

[8] Huang B, Clark G, Moratalla E N, Klein D R, Cheng R, Seyler K L, Zhong D, Schmidgall E, McGuire M A, Cobden D H, Yao W, Xiao D, Herrero P J and Xu X D 2017 *Nature* **546** 270

[9] Gong C, Li L, Li Z L, Ji H W, Stern A, Xia Y, Cao T, Bao W, Wang C Z, Wang Y, Qiu Z Q, Cava R J, Louie S G, Xia J and Zhang X 2017 *Nature* **546** 265

[10] Li X, Wu X and Yang J 2014 *J. Am. Chem. Soc.* **136** 11065

[11] Du K Z, Wang X Z, Liu Y, Hu P, Utama M I B, Gan C K, Xiong Q and Kloc C 2016 *ACS Nano* **10** 1738

[12] Klingen W, Eulenberger G and Hahn H 1970 *Naturwissenschaften* **57** 88

[13] Taylor B E, Steger J and Wold A 1973 *J. Solid State Commun.* **7** 461

[14] Jernberg P, Bjarman S and Wäppling R 1984 *J. Magn. Magn. Mater.* **46** 178

[15] Scagliotti M, Jouanne M, Balkanski M and Ouvrard G 1985 *J. Solid State Commun.* **54** 291

[16] Jouanne M, Sanjuan M L, Kanehisa M A, Balkanski M and Scagliotti M 1989 *Mater. Sci. Eng. B* **3** 85

[17] Flem G L, Brec R, Ouvrard G, Louisy A and Segransan P 1982 *J. Phys. Chem. Solids* **43** 455

[18] Rule K C, McIntyre G J, Kennedy S J and Hicks T J 2007 *Phys. Rev. B* **76** 134402

[19] Zhu W, Gan W, Muhammad Z, Wang C D, Wu C Q, Liu H J, Liu D B, Zhang K, He Q, Jiang H L, Zheng X S, Sun Z, Chen S M and Song L 2018 *Chem. Commun.* **54** 4481

[20] Lee J U, Lee S, Ryoo J H, Kang S, Kim T Y, Kim P, Park C H, Park J G and Cheong H 2016 *Nano Lett.* **16** 7433

[21] Cheng Z Z, Shifa T A, Wang F M, Gao Y, He P, Zhang K, Jiang C, Liu Q L and He J 2018 *Adv. Mater.* **30** 1707433

[22] Gao Y, Lei S J, Kang T T, Fei L F, Mak C L, Yuan J, Zhang M G, Li S J, Bao Q L, Zeng Z M, Wang Z, Gu H S and Zhang K 2018 *Nanotechnology* **29** 244001

[23] Zhang S, Zhao X D, Wu D H and Zhou Z 2016 *Adv. Sci.* **3** 1600062

[24] Kuo C T, Neumann M, Balamurugan K, Park H J, Kang S, Shiu H W, Kang J H, Hong B H, Han M, Noh T W and Park J G 2016 *Sci. Rep.* **6** 20904

[25] Murayama C, Okabe M, Urushihara D, Asaka T, Fukuda K, Isobe M, Yamamoto K and Matsushita Y 2016 *J. Appl. Phys.* **120** 142114

[26] Wang X Z, Du K Z, Liu Y Y F, Hu P, Zhang J, Zhang Q, Owen M H S, Lu X, Gan C K, Sengupta P, Kloc C and Xiong Q H 2016 *2D Mater.* **3** 031009

[27] Scagliotti M, Jouanne M, Balkanski M, Ouvrard G and Benedek G 1987 *Phys. Rev. B* **35** 7097

[28] Rehman Z U, Muhammad Z, Moses O A, Zhu W, Wu C, He Q, Habib M and Song L 2018 *Micromachines* **9** 292

[29] Wildes A R, Rule K C, Bewley R I, Enderle M and Hicks T J 2012 *J. Phys.: Condens. Matter* **24** 416004

[30] Joy P A and Vasudevan S 1992 *Phys. Rev. B* **46** 5425

[31] Mayorga-Martinez C C, Sofer Z, Sedmidubský D, Huber Š, Eng A Y S and Pumera M 2017 *ACS Appl. Mater. Interfaces* **9** 12563